

Highlights from the BESIII experiment

Isabella Garzia^{1,2,*}, on behalf of the BESIII Collaboration

¹University of Ferrara - Dipartimento di Fisica e Scienze della Terra, Ferrara, Italy

²Istituto Nazionale di Fisica Nucleare (INFN), Sezione di Ferrara, Ferrara, Italy

Abstract. Since 2009, the BESIII experiment has been collecting e^+e^- physics data in the energy range between 2.0 up to 4.95 GeV. This allowed the BESIII Collaboration to collect three of the largest data sets of charmonium J/ψ , $\psi(2S)$, and $\psi(3770)$ resonances in the world. In particular, the radiative decay of J/ψ provides a gluon-rich environment and it is therefore regarded as one of the most promising hunting grounds for glueballs, as well as a powerful tool for searching exotic states. In this proceeding, we present the first measurement of the quantum numbers of the $X(2370)$ particle, which shows very promising glueball features, and the first observation of exotic isoscalar state $\eta_1(1855)$ in the $J/\psi \rightarrow \gamma\eta\eta'$ decay. Latest studies on the $\eta(1405)/\eta(1474)$ are also reported, together with the observation of a new state, $X(1880)$, observed in the $J/\psi \rightarrow \gamma(3\pi^+\pi^-)$ decay. Finally, the normalized differential cross section of inclusive π^0 , K_S^0 , and η production as a function of hadron momentum are measured at several center of mass energies from 2.000 to 3.6710 GeV. The results deviates from several theoretical calculation based on existing fragmentation functions and provide new ingredient for global data fits.

1 Introduction

The Beijing Electron Spectrometer III (BESIII) detector [1] is a general purpose magnetic spectrometer installed at the Beijing Electron Positron Collider II (BEPCII) [2]. BEPCII is a symmetric double-ring e^+e^- collider hosted at the Institute of High Energy Physics with a beam energy tuneable in a range from 1.0 GeV to 2.45 GeV. The BESIII detector has a geometrical acceptance of 93% of 4π solid angle and it consists of four main subsystems: a helium-based multilayer drift chamber (MDC), a plastic scintillator time-of-flight (TOF) system, a CsI(Tl) electromagnetic calorimeter (EMC) and a resistive plate muon chamber. The first three subdetectors are enclosed in a superconductive solenoidal magnet which generates a magnetic field of about 1 T. More details can be found in [1].

The BESIII experiment has accumulated about 10 billion J/ψ events, about 2.7×10^9 $\psi(3686)$ events, and a total integrated luminosity of about 20 fb^{-1} at the center of mass energy of 3.773 GeV, that provide a clean laboratory to study light hadron physics and search for light exotic hadron states, such as multiquark states, glueballs and hybrids. Other data has been collected at several center of mass energy from 2 GeV up to 4.95 GeV, which allows to cover a very rich physics program in the so called τ -charm region.

*e-mail: isabella.garzia@unife.it, garzia@fe.infn.it

2 Glueballs and exotic hybrid states

The existence of glueballs has been predicted by Quantum Chromodynamics (QCD). According to Lattice QCD calculation [3–5], the mass of the ground state glueball with quantum number $J^{PC} = 0^{++}$, should be in the range [1.6-1.7] GeV/ c^2 , while the mass of the first excited state (with $J^{PC} = 2^{++}$) should be around 2.3 GeV/ c^2 . These mass ranges are accessible at the BESIII experiment. In addition to the high statistic collected, radiative J/ψ decay is a gluon rich process. Therefore, it is regarded as one of the most promising hunting grounds for glueballs.

QCD also allows the existence of hybrid mesons, $q\bar{q}$ states with gluonic degree of freedom. Models and Lattice QCD (LQCD) predict that the exotic $J^{PC} = 1^{-+}$ nonet hybrid mesons is the lightest, with a mass around 1.7 – 2.1 GeV/ c^2 [6]. To date, there are evidence of three isovector 1^{-+} states ($\pi_1(1400)$, $\pi_1(1600)$, and $\pi_1(2015)$) [7–10]. Finding an isoscalar 1^{-+} hybrid state is critical for establishing the hybrid multiplet.

2.1 Observation of exotic isoscalar state $\eta_1(1855)$ in $J/\psi \rightarrow \gamma\eta\eta'$

Based on a sample of $(10.09 \pm 0.04) \times 10^9$ J/ψ events collected by BESIII, a Partial Wave Analysis (PWA) of $J/\psi \rightarrow \gamma\eta\eta'$ to search for 1^{-+} and investigate the decay property of $f_0(1710)$ was performed [11, 12]. An isoscalar state with exotic quantum number 1^{-+} , denoted as $\eta_1(1855)$, has been observed for the first time with a statistical significance larger than 19σ . Its mass and width are measured to be $(1855 \pm 9_{-1}^{+6})$ MeV/ c^2 and $(188 \pm 18_{-8}^{+3})$ MeV [12], in agreement with LQCD calculation [13]. Figure 1 shows the PWA fit projection on the $\eta\eta'$ invariant mass distribution. In addition, the decay $J/\psi \rightarrow \gamma f_0(1500) \rightarrow \gamma\eta\eta'$ has also been observed with a statistical significance larger than 30σ , while the $J/\psi \rightarrow \gamma f_0(1710) \rightarrow \gamma\eta\eta'$ is found to be negligible. The suppressed decay rate of the $f_0(1710)$ into $\eta\eta'$ supports the hypothesis that the $f_0(1710)$ has a large overlap with the scalar glueball, and the $f_0(1710)/f_0(2020)$ might be interpreted as flavor singlet [14].

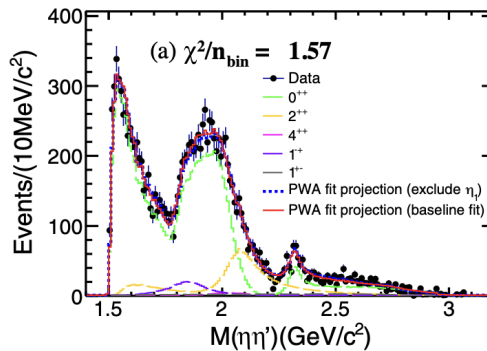


Figure 1. PWA fit projection for the invariant mass distribution of $\eta\eta'$. The red line is the total fit projections from the baseline PWA, while the blue dotted line represents the fit projection from a fit excluding the η_1 component.

2.2 The $\eta(1405)/\eta(1475)$ in $J/\psi \rightarrow \gamma K_S^0 K_S^0 \pi^0$ decay and $J/\psi \rightarrow \gamma\gamma\phi$

Radiative J/ψ decay can also be used to investigate the nature of the pseudoscalar structure around 1.4 GeV/ c^2 , which is often interpreted as the combination of two isoscalar resonant

state, i.e., the $\eta(1405)$ and $\eta(1475)$. From a theoretical point of view, the pseudoscalar nonet of ground state is well established, and the $\eta(1295)$ and $\eta(1475)$ are generally assigned to be the first radial excitation of the ground state η and η' [32], and hence it became very difficult to accommodate additional pseudoscalar states. Therefore, the possibility of an additional unconventional state has been widely discussed. To investigate the $\eta(1405/1475)$ nature, BESIII Collaboration performed a PWA analysis of the decay $J/\psi \rightarrow \gamma K_S^0 K_S^0 \pi^0$ using the full J/ψ data set, where both mass dependent (MD) and mass independent (MI) approach are performed [16]. In particular, to extract the contributions from different components, a MI PWA is performed: the intermediate states in the $K_S^0 K_S^0 \pi^0$ invariant mass spectrum are parameterized by a separate complex constant in 24 bins of $15 \text{ MeV}/c^2$ width in the region $M(K_S^0 K_S^0 \pi^0) < 1.6 \text{ GeV}/c^2$ (bin-by-bin analysis). Taking into account the spin-parity, charge conjugation and isospin conservation, all possible decay mode candidates are evaluated, and the $K_S^0 K_S^0 \pi^0$ invariant mass spectra obtained from the MI PWA results are shown in Figure 2. The fit results confirm that the dominant contribution comes from the pseudoscalar component; axial vector component also contribute (peaking at $1.28 \text{ GeV}/c^2$ and $1.42 \text{ GeV}/c^2$); and there is also a small tensor component decaying into $K^*(892)^0 K_S^0$ around $1.52 \text{ GeV}/c^2$ observed for the first time in this decay mode. A mass dependent PWA is also performed, and the results are summarized in Ref. [16]. The nominal solution is in good agreement with the MI PWA results, and it includes two pseudoscalar state, the $\eta(1405)$ and the $\eta(1475)$, two axial vector states, the $f_1(1285)$ and the $f_1(1425)$, and a tensor state, the $f_2(1525)$.

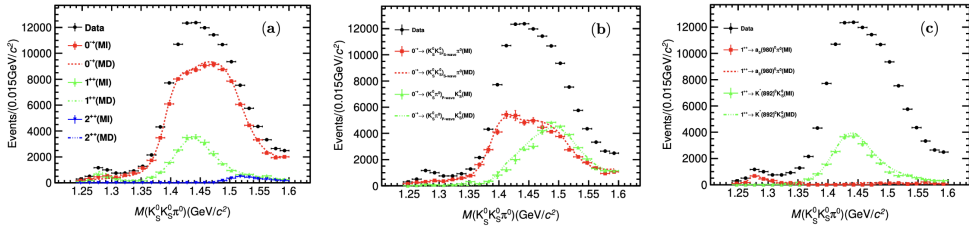


Figure 2. Intensity spectra of $K_S^0 K_S^0 \pi^0$ invariant mass distribution: (a) dominant spin-parity components, (b) dominant decay modes for the pseudoscalar component, and (c) dominant decay modes for the axial vector component. Dots with error bars are the intensity obtained from the MI PWA, while the dotted lines are obtained from MD PWA results.

For the first time, in a recent BESIII analysis was performed a PWA of the decay $J/\psi \rightarrow \gamma\gamma\phi$, which serve as flavor filter reaction and play a important role in the investigation of the quark contents of the intermediate resonances [17]. The PWA result shows that the $J/\psi \rightarrow \gamma X; X \rightarrow \gamma\phi$ process has predominantly 2^{++} components. The $\eta(1405)$, $X(1835)$, and several f-states are observed with a statistical significance greater than 5σ . In particular, the structure with mass around $1.4 \text{ GeV}/c^2$ in the $\gamma\phi$ system is described taking into account the $\eta(1405)$ and $f_1(1420)$ contributions. These results indicate that only one pseudoscalar state is needed in the vicinity of $1.4 \text{ GeV}/c^2$. In addition, the quantum number of the $X(1835)$ are confirmed to be 0^{-+} , and its observation decaying into $\gamma\phi$ final state indicates that this resonance also contains a sizable $s\bar{s}$ component.

2.3 $X(2370)$: Glueball-like particle in $J/\psi \rightarrow \gamma K_S^0 K_S^0 \eta'$

The $X(2370)$ resonance was first observed in the $J/\psi \rightarrow \gamma\pi^+\pi^-\eta'$ process in the $\pi^+\pi^-\eta'$ invariant mass distribution [18], and it was further observed in a combined measurement of

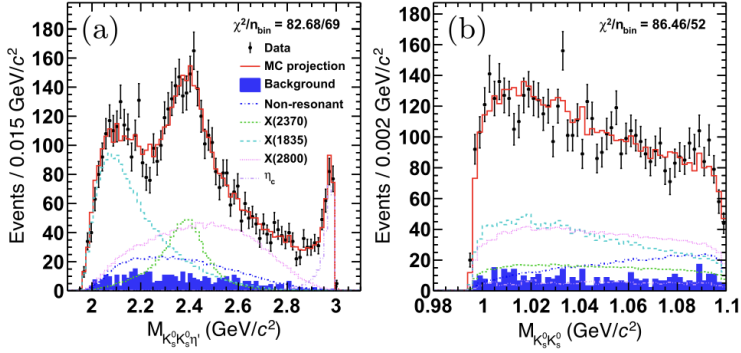


Figure 3. PWA fit projections on the (a) $K_S^0 K_S^0 \eta'$ and (b) $K_S^0 K_S^0$ invariant mass distributions. Dots with error bars refer to data, solid red histograms are the PWA total projections.

$J/\psi \rightarrow \gamma K^+ K^- \eta'$ and $J/\psi \rightarrow \gamma K_S^0 K_S^0 \eta'$ [19]. These experimental observation stimulated several theoretical interpretations on its nature. Among them, one of the most promising explanation is a pseudoscalar glueball [20–22]. To understand the nature of the $X(2370)$, it is crucial to measure the quantum numbers and the decay modes, and the $J/\psi \rightarrow \gamma K_S^0 K_S^0 \eta'$ decay provides a clean environment for the J^{PC} measurement with minimal background contamination due to the fact that the main background processes, $J/\psi \rightarrow \pi^0 K_S^0 K_S^0 \eta'$ and $J/\psi \rightarrow K_S^0 K_S^0 \eta'$, are forbidden by exchange symmetry and CP conservation. Using the full J/ψ data set collected at BESIII, the spin-parity determination of the $X(2379)$ was obtained for the first time [23]. A strong enhancement near the $K_S^0 K_S^0$ mass threshold from the $f_0(980)$ was observed, together with a clear connection between the $f_0(980)$ and the structure around 2.4 GeV/c^2 in the invariant mass spectra of $K_S^0 K_S^0 \eta'$. After requiring the $K_S^0 K_S^0$ invariant mass to be less than 1.1 GeV/c^2 , the structure around 2.4 GeV/c^2 becomes much more prominent in the $K_S^0 K_S^0 \eta'$ mass spectrum. A PWA fit is performed in order to study the properties of the $X(2370)$ state, and the optimal PWA fit results, shown in Figure 3, shows that the data can be well described taking into account the following intermediate states: $X(1835)$, $X(2370)$, η_c , and a broad 0^{++} structure denoted as $X(2800)$. The PWA fit result indicates a contribution from $X(2370) \rightarrow K_S^0 K_S^0 \eta'$ with a statistical significance larger than 14σ , with the mass and width of the $X(2370)$ measured to be $2395 \pm 11(\text{stat})^{+26}_{-94} \text{ MeV}/c^2$ and $188^{+18}_{-17}(\text{stat})^{+124}_{-33} \text{ MeV}$, respectively. The spin parity of the $X(2370)$ is determined to be 0^{++} for the first time. In addition, the measured mass is in good agreement with the mass prediction of the lightest pseudoscalar glueball [20], which makes the $X(2370)$ state a promising glueball candidate.

2.4 $X(1880)$: A new state observed in $J/\psi \rightarrow \gamma(3\pi^+ \pi^-)$

The $X(1835)$ resonance was first observed in the $\pi^+ \pi^- \eta'$ invariant mass spectrum [24] and as a $p\bar{p}$ threshold enhancement in the $J/\psi \rightarrow \gamma p\bar{p}$ decay [25] at BESIII. Its nature is still controversial and several theoretical models are proposed. The $X(1835)$ was later confirmed by BESIII [26] and CLEO [27] experiments, and the quantum number measured to be 0^{++} [28]. Meanwhile, a prominent structure, named as $X(1840)$, was observed in the $3(\pi^+ \pi^-)$ invariant mass spectrum [29]. Even if it was interpreted as a new decay mode of the $X(1835)$, its width is substantially narrower than that of $X(1835)$.

In an updated analysis of $J/\psi \rightarrow \gamma \pi^+ \pi^- \eta'$ is observed a significant abrupt change in the slope of the $X(1835) \rightarrow \pi^+ \pi^- \eta'$ line shape at the $p\bar{p}$ mass threshold [30], which could

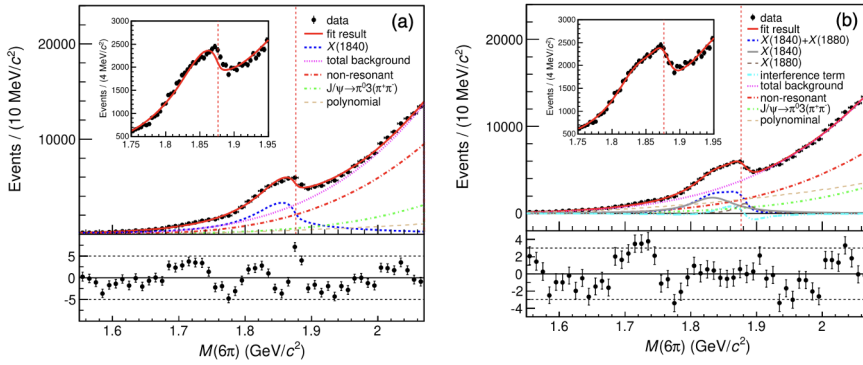


Figure 4. Fit result of the 6π invariant mass distribution ($M(6\pi)$) for model-I (a) and model-II (b).

be originated from the opening of an additional $p\bar{p}$ decay channel or the interference between two different resonance contributions. It is interesting to understand whether a similar phenomenon exists around the $p\bar{p}$ mass threshold in the 6π invariant mass distribution by analysing the $X(1840)$ line shape in the $J/\psi \rightarrow \gamma 3(\pi^+\pi^-)$ decay [31]. After the event and track selection, discussed in detail in ref. [31], an anomalous line shape near the $p\bar{p}$ mass threshold is clearly observed, and an unbinned maximum likelihood fit to the 6π invariant mass spectrum ($M(6\pi)$) was performed. When the $X(1840)$ is described as a simple resonant structure, the fit quality is very poor: a simple resonance structure cannot be used to describe the $M(6\pi)$ spectrum. To resolve the discrepancy from data, two different models for the line shape of the structure around the $p\bar{p}$ structure are investigated. In model-I, it was assumed that the change in the line shape of 6π above the $p\bar{p}$ mass threshold is due to the opening of the $X(1840) \rightarrow p\bar{p}$ decay, and the anomalous shape is described with a Flatté formula. Figure 4 (a) shows the comparison between the data and the fit result of model-I, where it is clearly visible a tension between data and fit results around the $p\bar{p}$ mass threshold. In order to obtain a better description of data, a second model (model-II) was taken into account: it allows the interference between two resonant structures, denoted as $X(1840)$ and $X(1880)$. As reported in Figure 4 (b), model-II improves the fit quality, and the $X(1880)$ is observed with a statistical significance larger than 10σ . According to the model-II fit results, the narrow structure $X(1880)$ has a mass of $M_{X(1880)} = 1882.1 \pm 1.7 \pm 0.7 \text{ MeV}/c^2$ and a width of $\Gamma_{X(1880)} = 30.7 \pm 5.5 \pm 2.4 \text{ MeV}$, while the mass and the width of $X(1840)$ are measured to be $M_{X(1840)} = 1832.5 \pm 3.1 \pm 2.5 \text{ MeV}/c^2$ and $\Gamma_{X(1840)} = 80.7 \pm 5.2 \pm 7.7 \text{ MeV}$. Compared with the two structures observed in the $\pi^+\pi^-\eta'$ mass spectrum [30], the $X(1840)$ has a mass consistent with that of the $X(1835)$ state but much narrower width, while the mass and width of the $X(1880)$ are in agreement with those reported in [30]. However, to establish the nature of these states, the determination of the spin-parity quantum numbers and couple channel amplitude analysis are needed.

3 Unpolarized fragmentation function at BESIII

Fragmentation Functions (FFs) are non-perturbative functions used to describe the hadronization of partons (quarks and gluons) into color-neutral particles. A precise knowledge of FFs will help to understand the color confinement property of the QCD at long distance, as well as they play a fundamental role in constraining the proton spin configuration and the nuclear

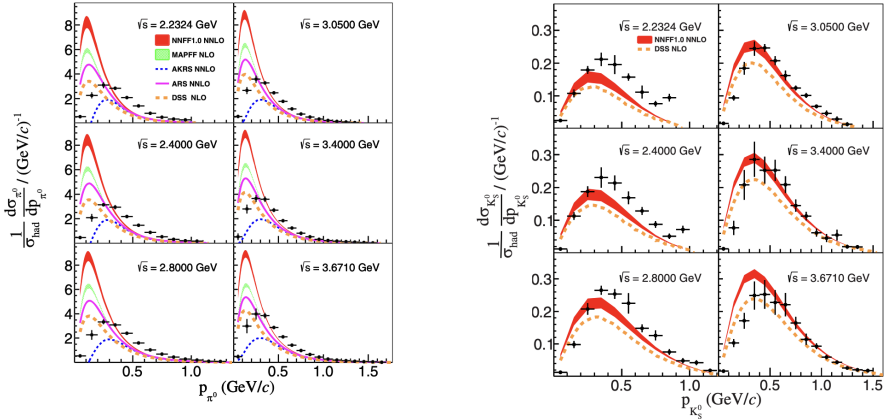


Figure 5. Normalised differential cross section of the $e^+e^- \rightarrow \pi^0 + X$ (left) and $e^+e^- \rightarrow K_S^0 + X$ (right) processes. Points with error bars refer to data, for which the uncertainties are the quadrature sum of the corresponding statistical and systematic uncertainties. The coloured bands denote several theoretical calculation [33].

parton distribution functions (PDFs). Single inclusive e^+e^- annihilation, $e^+e^- \rightarrow h+X$, where h is an identified hadron and X represents everything else, provides a clean laboratory to study the unpolarized FFs. Here, the dimensionless variable $z = 2E_h / \sqrt{s}$ is the relative hadron energy, E_h is the hadron energy, and \sqrt{s} is the center of mass energy. A typical experimental observable is

$$\frac{1}{\sigma(e^+e^- \rightarrow \text{hadrons})} \frac{d\sigma(e^+e^- \rightarrow h + X)}{dp_h},$$

where $\sigma(e^+e^- \rightarrow \text{hadrons})$ is the total cross section for e^+e^- annihilation to all possible hadronic final states, and p_h denotes the momentum of the identified hadron h . The observable can be interpreted, in terms of the leading order α_s , as $\sum_q e_q^2 [D_q^h(z, \sqrt{s}) + D_{\bar{q}}^h(z, \sqrt{s})]$, where e_q is the fractional charge of the quark q , and $D_{q(\bar{q})}^h(z, \sqrt{s})$ is the unpolarized FF of quark q (anti-quark \bar{q}) at \sqrt{s} .

As summarised in Ref. [32], several high-precision measurements of unpolarized FFs have been made in e^+e^- annihilation experiments at the center of mass energy above 10 GeV, while few data with huge statistical uncertainties are present in the energy region from 3.6 to 5.2 GeV. Using the BESIII data collected at six center of mass energies from 2.2324 to 3.6710 GeV, the processes $e^+e^- \rightarrow \pi^0/K_S^0 + X$ are studied [33]. The normalised differential cross sections for the inclusive π^0 and K_S^0 production are shown in Figure 5 together with various theoretical predictions extrapolated from different FFs determined from existing world data [32]. The results provide broad z coverage from 0.1 to 0.9. For both π^0 and K_S^0 , it is clear the discrepancy between data and theoretical prediction, which is observed to depend on both the hadron momentum and \sqrt{s} . One possible explanation of this discrepancies is that the theoretical prediction, restricted to the leading twist contribution, it is not sufficient at the BESIII energy scale. It may also be important to consider quark mass and hadron mass correction effects and small- z resummation effects, as well as the fact that the theoretical models are obtained from existing e^+e^- annihilation at high energy scale and then extrapolated to the low-energy scale of BESIII. However, these results provide new ingredient for global data analyses.

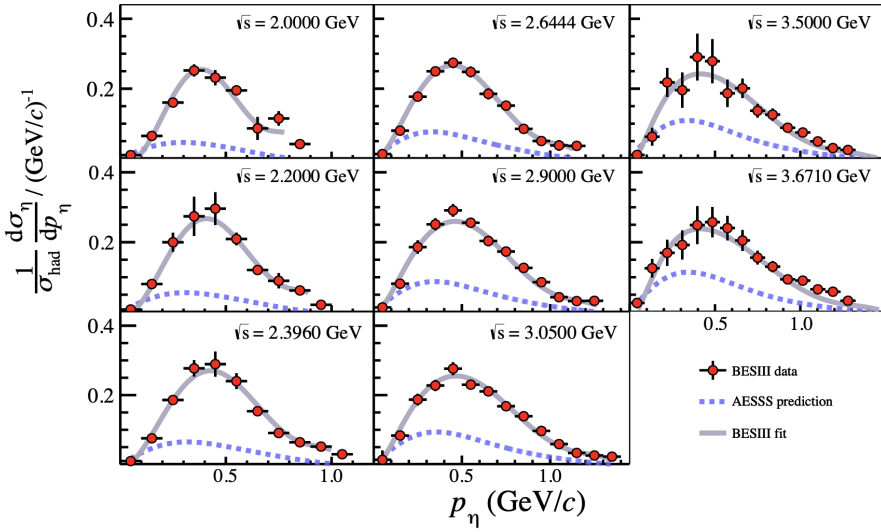


Figure 6. Normalised differential cross sections of the $e^+e^- \rightarrow \eta + X$ process. The blue dotted curves denote the prediction by using the AESSS FFs [35], while the grey curves denote the calculations by using the newly extracted η FFs from BESIII.

In addition to π^0/K_S^0 , for the first time, BESIII reports the measurement of the process $e^+e^- \rightarrow \eta + X$ at eight \sqrt{s} from 2.0000 to 3.6710 GeV, with a z coverage from 0.3 to 0.9 [34]. The normalised differential cross sections for the inclusive η production are shown in Figure 6. The blue dotted curves in Figure 6 represent the theoretical prediction obtained by using the η FF from AESSS parameterization [35] extracted using data of η production in e^+e^- annihilation with $\sqrt{s} > 10$ GeV. The disagreement with BESIII data is evident.

The grey line in Figure 6 shows a new calculation [34] in which also the new η BESIII data are considered. In this case, the model describes the data better. These new results in the relatively low energy region provide special ingredients for FF studies, and they will help to enhance our understanding of the QCD factorization theorem at the leading twist and beyond.

4 Conclusion

The BESIII Collaboration started taking physics data in 2009, and a lot of new physics results are obtained since then. The main focus of this proceeding is the report of the most recent results of the BESIII Collaboration in the QCD field. In particular, thanks to the world largest J/ψ data sample collected by BESIII, a dedicated program on the light hadron spectroscopy and decays has allowed to investigate the nature of the light hybrids, glueball states, and mesonic molecules. In addition to the J/ψ data, data collected at \sqrt{s} from 2.0000 to 3.6710 GeV are used to extract the normalised differential cross section for several inclusive hadrons production. Such studies will be fundamental to a better understanding of fragmentation processes and shed light on the QCD factorization theorem, as well as non-perturbative processes. Finally, new upgrade on the BEPCII collider and on the BESIII detector planned by the end of the 2024 will open new interesting scenario.

References

- [1] Ablikim M., et al. (BESIII Collaboration), Nucl. Instrum. Methods Phys. Res., Sect. A **614**, 345 (2010), Design and Construction of the BESIII Detector
- [2] Yu C. H., et al. in Proceedings of IPAC2016, Busan, Korea, p.p 1012-1018
- [3] Bali G. S., Schilling K., Hulsebos A., Irving A., Michael C., and Stephenson P. W. Phys. Lett. B **309** 378 (1993)
- [4] Morningstar C. J. and Peardon M. J., Phys. Rev. D **60**, 034509 (1999)
- [5] Gregory E., Irving A., Luciani B., McNeile C., Rago A., Richards C., and Rinaldi E., J. High Energy Phys. **10**, 170 (2012)
- [6] Meyer C. A., and Swanson E. S., Prog. Part. Nucl. Phys. **82**, 21 (2015)
- [7] Mayer C. A., and Van Haarlem Y., Phys. Rev. C **82**, 025208 (2010)
- [8] Klempt E., and Zaitsev A., Phys. Rep. **454**, 1 (2007)
- [9] Rodas A., et al., (JPAC Collaboration), Phys. Rev. Lett. **122**, 042002 (2019)
- [10] Woss A. J., et al. (Hadron Spectrum Collaboration) Phys. Rev. D **103**, 054503 (2021)
- [11] Ablikim M., et al. (BESIII Collaboration), Phys. Rev. L **129**, 192002 (2022)
- [12] Ablikim M., et al. (BESIII Collaboration), Phys. Rev. D **106**, 072012 (2022); Phys. Rev. D **107**, 079901 (2023)
- [13] Dudek J. J., Edwards R. G., Guo P., Thomas C. E. (Hadron Spectrum Collaboration), Phys. Rev. D **88**, 094505 (2013)
- [14] Klempt E., and Sarantev A. V., Phys. Lett. B **826**, 136906 (2022)
- [15] Zyla P. A., et al. (Particle Data Group), Prog. Theor. Exp. Phys. **2020**, 083C01 (2020)
- [16] Ablikim M., et al. (BESIII Collaboration), JHEP **03**, 121 (2023)
- [17] Ablikim M., et al. (BESIII Collaboration), arXiv:2401.00918 <https://arxiv.org/pdf/2401.00918>
- [18] Ablikim M., et al. (BESIII Collaboration), Phys. Rev. L **106**, 072002 (2011)
- [19] Ablikim M., et al. (BESIII Collaboration), Eur. Phys. J. C **80**, 746 (2020)
- [20] L.-C. Gui, J.-M. Dong, Y. Chen, and Y.-B. Yang, Phys. Rev. D **100**, 054511 (2019)
- [21] W. I. Eshraim, S. Janowski, F. Giacosa, and D. H. Rischke, Phys. Rev. D **87**, 054036 (2013)
- [22] R. Zhang, W. Sun, Y. Chen, M. Gong, L.-C. Gui, and Z. Liu, Phys. Rev. B **827**, 136960 (2022)
- [23] Ablikim M., et al. (BESIII Collaboration), Phys. Rev. Lett. **132**, 181901 (2024)
- [24] Ablikim M., et al. (BESIII Collaboration), Phys. Rev. Lett. **95**, 262001 (2005)
- [25] J. Z. Bai, et al. (BES Collaboration), Phys. Rev. Lett. **91**, 022001 (2003)
- [26] Ablikim M., et al. (BESIII Collaboration), Phys. Rev. Lett. **106**, 072002 (2011)
- [27] J. P. Alexander, et al. (CLEO Collaboration), Phys. Rev. D **82**, 092002 (2010)
- [28] Ablikim M., et al. (BESIII Collaboration), Phys. Rev. Lett. **115**, 091803 (2015)
- [29] Ablikim M., et al. (BESIII Collaboration), Phys. Rev. D **88**, 091502 (2013)
- [30] Ablikim M., et al. (BESIII Collaboration), Phys. Rev. Lett. **117**, 042002 (2016)
- [31] Ablikim M., et al. (BESIII Collaboration), Phys. Rev. Lett. **132**, 151901 (2024)
- [32] Navas S., et al. (Particle Data Group), Phys. Rev. D **110**, 030001 (2024)
- [33] Ablikim M., et al. (BESIII Collaboration), Phys. Rev. Lett. **130**, 231901 (2023)
- [34] Ablikim M., et al. (BESIII Collaboration), arXiv:2401.17873 <https://arxiv.org/pdf/2401.17873>
- [35] Aidala C. A., et al., Phys. Rev. D **83**, 034002 (2011)